Krüppel-like factor 4 ameliorates diabetic kidney disease by activating autophagy via the mTOR pathway

JIANGUANG GONG[1-3], HUIFANG ZHAN[4], YIWEN LI[1-3], WEI ZHANG[1-3], JUAN JIN[1-3] and QIANG HE[1-3]

[1]Department of Nephrology, Zhejiang Provincial People's Hospital; [2]People's Hospital of Hangzhou Medical College;
[3]Chinese Medical Nephrology Key Laboratory of Zhejiang Province, Hangzhou, Zhejiang 310014;
[4]Department of Emergency, Zhejiang University Hospital, Hangzhou, Zhejiang 310058, P.R. China

Abstract. Diabetic kidney disease (DKD) is diagnosed increasingly frequently and represents a serious threat to human health. Krüppel-like factor 4 (KLF4) has aroused attention due to its potential effect on podocytes and in ameliorating proteinuria associated with glomerulopathy. The purpose of the present study was to investigate the potential role of KLF4 in DKD. It was hypothesized that KLF4 impacts diabetic nephropathy by mediating the podocyte autophagic process. A KLF4 plasmid vector was constructed, and podocytes were transfected and incubated with DKD mice serum for *in vitro* experiments. A db/db spontaneous DKD mouse model was also established for *in vivo* study. After treatment, the level of serum creatinine (Scr), blood urea nitrogen (BUN), and 24-h urinary protein was determined. Immunofluorescence and periodic acid-Schiff staining, western blotting, flow cytometry and a TUNEL assay were performed to observe changes in glomerular morphology and the level of apoptosis, cytoskeleton proteins, epithelial-mesenchymal transition (EMT) biomarkers, autophagic proteins and mTOR pathway proteins in each group. KLF4 overexpression significantly reduced the level of urinary albumin, Scr, BUN and attenuated mesangial matrix expansion, as well as mesangial cell proliferation in DKD mice. KLF4 overexpression also inhibited podocyte apoptosis and downregulated vimentin and α-smooth muscle actin, and upregulated E-cadherin and nephrin, both *in vivo* and *in vitro*. Moreover, the microtubule associated protein 1 light chain 3α (LC3)-II/LC3-I ratio and LC3-II fluorescence was significantly increased in the vector-KLF4 group compared to the negative control vector group both *in vivo* and *in vitro*. Finally, a decrease in the level of phosphorylated (p)-mTOR and p-S6K protein expression was observed following KLF4 overexpression *in vitro*. The present findings suggested that KLF4 plays a renoprotective role in DKD, which is associated with the activation of podocyte autophagy, and may be involved in the mTOR signaling pathway.

Introduction

Diabetic kidney disease (DKD) is increasingly diagnosed and has become a leading cause of end-stage renal disease (ESRD) throughout the world during the past few decades (1,2). DKD is characterized by mesangial expansion, a thicker glomerular basement membrane, progressive glomerulosclerosis, and finally the development of progressive fibrosing kidney disease. Previous studies have demonstrated that several pathological factors are involved in the progression of diabetic nephropathy (DN), including the downregulation of autophagy (3), podocyte apoptosis, detachment (4) and epithelial-mesenchymal transition (EMT) (5); however, the precise mechanism remains elusive. Therefore, exploring the precise mechanism and identifying effective strategies for the treatment of DN remains crucial.

Recently, Krüppel-like factor 4 (KLF4), a zinc finger-containing transcription factor, has aroused attention due to its potential effect on podocyte and kidney disease. KLF4 belongs to the family of SP/KLF factors and plays a crucial role in regulating various cellular processes (e.g., cell growth, proliferation, differentiation, and inflammation) (6). A recent study revealed that endothelial KLF4 is renoprotective and mediates statin-induced protection against ischemic AKI by regulating the expression of cell adhesion molecules and the concomitant recruitment of inflammatory cells (7). In addition, Hayashi *et al* (8) confirmed that KLF4 is expressed in podocytes and found that KLF4 overexpression resulted in a sustained increase in nephrin expression and a decrease in albuminuria, both in animal models and humans exhibiting proteinuria. These findings suggest that KLF4 has a renoprotective effect on chronic renal disease; however, little is known about the specific mechanism.

In the present study, a KLF4 plasmid vector was constructed, and a db/db spontaneous DKD mouse model, as well as DKD mouse serum-induced podocyte injury, were utilized to explore the potential role of KLF4 in DN and its underlying mechanism.

Correspondence to: Dr Juan Jin or Dr Qiang He, Department of Nephrology, Zhejiang Provincial People's Hospital, 158 Shangtang Road, Xiacheng, Hangzhou, Zhejiang 310014, P.R. China
E-mail: lang_018@163.com
E-mail: qianghe1973@126.com

Materials and methods

Cell culture and grouping. Conditionally immortalized differentiated mouse podocytes (MPC5) were purchased from the Institute of Basic Medicine at the Chinese Academy of Medical Sciences. The cells were cultured as described previously (9). Briefly, to induce proliferation, the cells were cultured at 33°C in RPMI 1640 medium (cat. no. SH30809.01B; HyClone; GE Healthcare Life Sciences) supplemented with 10% fetal bovine serum (FBS), 100 U/ml penicillin G, 100 mg/ml streptomycin and 100 U/ml interferon (IFN)-γ. To promote differentiation, the cells were cultured in medium without IFN-γ at 37°C. The differentiated podocytes were diluted for all subsequent experiments. Podocytes were divided into four groups: i) Control serum group (treated with 10% serum from C57BL/KsJ db/m mice for 24 h); ii) DKD serum group (treated with 10% serum from C57BL/KsJ db/db mice for 24 h); iii) DKD serum + Vector-negative control (NC) group (transfected with an empty plasmid for 72 h following treatment with DKD mouse serum); and iv) DKD serum + Vector-KLF4 group [transfected with the pcDNA3.1(+)-KLF4 plasmid for 72 h following treatment with DKD mouse serum].

Animals and grouping. Male C57BL/KsJ db/db spontaneous DKD model mice (n=10; 8 weeks old; weight, 22.3-26.5 g) and C57BL/KsJ db/m control mice (n=5; 8 weeks old; weight, 20.8-24.1 g) were obtained from Cavens Experimental Animal Co., Ltd. As previously described (10), mice were bred in a 12-h light/dark cycle in a pathogen-free facility at a constant temperature (20±2°C) and humidity (50-60%) with free access to food (a standard diet) and water for 5 weeks. C57BLKS/J db/db mice at 13 weeks old were randomly assigned to one of two groups: i) db/db + vector-NC group (n=5; receiving an injection of 5x10^8 IU lentiviral vector-NC every 5 days for 30 days); and ii) db/db + vector-KLF4 group (n=5; receiving an injection of 5x10^8 IU lentiviral vector-KLF4 every 5 days for 30 days). Age-matched db/m mice (n=5) were used as the control group. No mice succumbed during the experiment. All mice were sacrificed and used for subsequent experiments.

KLF4 vector construction and transfection. The synthetic gene fragments of KLF4 (synthesized by Shanghai Jierui Biological Engineering Co., Ltd.) were incorporated into a plasmid (pcDNA3.1; cat. no. V79020; Invitrogen; Thermo Fisher Scientific, Inc.) following double enzyme digestion with *Nhe*I-*Bam*HI (cat. nos. D1162A and D1010A; Takara Biotechnology Co., Ltd.), and termed pcDNA3.1(+)-KLF4. The products were transformed into DH5α-competent cells (cat. no. CD201-01; Beijing TransGen Biotech Co., Ltd.), smeared on a lysogeny broth (LB) ampicillin (AMP) plate, and cultured at 37°C overnight. An LB culture solution containing AMP was used to screen for the objective colonies. MPC5 cells were transfected with 800-1,500 ng/μl pcDNA3.1(+)-KLF4 using Lipofectamine® 2000 (Invitrogen; Thermo Fisher Scientific, Inc.) for 72 h, according to the manufacturer's instructions.

The synthetic gene fragments of KLF4 were cloned into a pCDH-CMV-MCS-EF1-GFP-Puro lentiviral vector (cat. no. CD511B-1; System Biosciences). The constructs (1.5 μg) were then transfected into 1x10^6/ml 293T cells (cat. no. CL-0005; Procell Life Science & Technology Co.,

Ltd.) using Lipofectamine 2000 (Invitrogen; Thermo Fisher Scientific, Inc.) according to the manufacturer's instructions. After 72 h, the lentivirus was collected. Mice were injected with 5x10^8 IU lentiviral vector-KLF4 every 5 days for 30 days through the tail vein after the DKD model had been successfully established.

Biochemical measurements. Urine collection was performed in metabolic cages at 13 weeks before treatment and 30 days after vector-KLF4 injection. Urine albumin was detected using an automatic biochemical analyzer (Hitachi 7020; Hitachi, Ltd.). The concentration of serum creatinine (Scr) and blood urea nitrogen (BUN) was detected using a creatinine assay kit (cat. no. C011-1; Nanjing Jiancheng Bioengineering Institute) and a urea nitrogen assay kit (cat. no. C013-2; Nanjing Jiancheng Bioengineering Institute), respectively.

Periodic acid-Schiff (PAS) staining. Kidney samples were fixed in 10% neutral-buffered formalin at room temperature for 12 h, embedded in paraffin wax and cut into 4-μm thick sections. Kidney sections from the mice were oxidized in 1% periodic acid for 10 min and washed with distilled water after being dewaxed. The tissues were then stained with Schiff's reagent (cat. no. G1281; Beijing Solarbio Science & Technology Co., Ltd.) for 10-20 min and washed again. Afterwards, the sections were counterstained in Harris's hematoxylin for 5-10 min. All steps were performed at room temperature. The images were observed under a light microscope (magnification, x400; DM2500; Leica Microsystems GmbH).

Immunofluorescence staining. MPC5 cells from the different treatment groups groups were seeded onto glass cover slips and fixed in 4% paraformaldehyde for 30 min at room temperature, then treated with phosphate buffered saline (PBS) supplemented with 0.1% Triton X-100 for 10 min at room temperature. Tissue sections were blocked with PBS containing 5% BSA (cat. no. SH30574.03; HyClone; GE Healthcare Life Sciences) for 1 h at room temperature after deparaffinization using xylene (cat. no. 1330-20-7; Shanghai Macklin Biochemical Co., Ltd.). The podocytes and tissue sections were incubated with the following primary antibodies at 4°C overnight: Anti-LC3 (Abcam; cat. no. ab192890; 1:500), anti-nephrin (cat. no. sc-377246; 1:50; Santa Cruz Biotechnology, Inc.), anti-filamentous (F-)actin (cat. no. ab130935; 1:100; Abcam), and anti-vimentin (cat. no. ab92547; 1:100; Abcam). After washing, the samples were incubated with Alexa Fluor 594-conjugated goat anti-rabbit IgG (cat. no. 111585003; 1:100; Jackson ImmunoResearch Inc), FITC-conjugated goat anti-mouse IgG (cat. no. A0568; 1:100; Beyotime Institute of Biotechnology), and Cy3-conjugated goat anti-rabbit IgG at 37°C for 1 h, followed by counterstaining with DAPI (1:500; Beyotime Institute of Biotechnology) at room temperature for 5 min. Images were observed under a laser scanning confocal fluorescence microscope (magnifications, x100 and x400; UltraVIEW VoX; PerkinElmer, Inc.).

Western blot analysis. The cells were lysed with cell lysis buffer (cat. no. P0013B; Beyotime Institute of Biotechnology) supplemented with protease cocktail (cat. no. 89806; Invitrogen; Thermo Fisher Scientific, Inc.) after washing three

times. Animal tissues were homogenized in RIPA lysis buffer and centrifuged for 5 min at 12,000 x g at 4°C. The protein concentration was quantified using a bicinchoninic acid assay. The proteins (30 μg/lane) were resolved by 8-12% SDS-PAGE and transferred onto PVDF membranes (EMD Millipore). The membranes were blocked at room temperature with 5% milk in TBS with Tween-20 for 1 h, and then probed with the following primary antibodies: Anti-KLF4 (cat. no. ab129473, 1:2,000; Abcam), anti-caspase-3 (cat. no. 9662; 1:1,000; Cell Signaling Technology, Inc.), anti-phosphorylated (p)-mTOR (cat. no. AF3308; 1:1,000; Affinity Biosciences), anti-mTOR (cat. no. AF6308; 1:1,000; Affinity Biosciences), anti-S6K (cat. no. AF6226; 1:500; Affinity Biosciences), anti-p-S6K (cat. no. AF3228; 1:500; Affinity Biosciences), anti-E-cadherin (cat. no. AF013; 1:1,000; Affinity Biosciences), anti-vimentin (cat. no. AF7013; 1:1,000; Affinity Biosciences), anti-α-smooth muscle actin (SMA; cat. no. AF1032; 1:500; Affinity Biosciences), anti-microtubule associated protein 1 light chain 3α (LC3; cat. no. 4108S; 1:1,000; Cell Signaling Technology, Inc.), anti-p62 (cat. no. 18420-1-AP; 1:500; ProteinTech Group, Inc.) and anti-β-actin (cat. no. 4970; 1:1,000; Cell Signaling Technology, Inc.) overnight at 4°C. The membranes were then incubated with HRP-conjugated goat anti-rabbit IgG antibody (cat. no. A0208; 1:1,000; Beyotime Institute of Biotechnology) or HRP-conjugated goat anti-mouse IgG antibody (cat. no. A0216; 1:1,000; Beyotime Institute of Biotechnology) for 1 h at room temperature after being washed with TBS. The blots were then visualized using an enhanced chemiluminescence reagent (cat. no. WBKLS0100; EMD Millipore) and analyzed using ImageJ software, version 1.8.0-112 (National Institutes of Health).

Analysis of apoptosis by flow cytometry and TUNEL assay. The ratio of apoptotic cells was determined using a fluorescein isothiocyanate-Annexin V Apoptosis Detection kit (BD Biosciences). The analysis was performed as previously described (9). Briefly, the cells were stained with FITC-Annexin V and propidium iodide, according to the manufacturer's instructions. Podocyte apoptosis was determined by flow cytometry (FACSCalibur; BD Biosciences) and analyzed using Accuri C6 software (version 1.0.264.21; BD Biosciences). The presence of apoptotic cells in the tissue sections was determined using a TUNEL Apoptosis kit (cat. no. BA27A; Nanjing Biobox Biotech Co., Ltd.), according to the manufacturer's instructions. After deparaffinization, sections of kidney tissue were decomposed with protease K and successively incubated in terminal transferase buffer with streptavidin-FITC-conjugated antibodies and a POD-conjugated anti-FITC solution, followed by staining with a diaminobenzidine solution (all in the TUNEL kit). Apoptotic cells were observed under a light microscope in five fields of view (magnification, x400; DM2500; Leica Microsystems GmbH).

Statistical analysis. All statistical analyses were performed using SPSS 21.0 software (IBM Corp.). Data are presented as the mean ± standard deviation. A multi-way ANOVA and one-way ANOVA followed by a least significant difference test were used to analyze the differences between multiple groups in the *in vitro* and *in vivo* experiments, respectively. P<0.05 was considered to indicate a statistically significant difference.

Results

Protective effect of KLF4 on podocytes treated with DKD mouse serum. To determine the role of KLF4 in podocytes growing in a high glucose environment, a plasmid encoding KLF4 (pcDNA3.1 + KLF4) and an empty vector were constructed and transfected into podocytes treated with DKD mouse serum. Western blotting revealed that the level of KLF4 expression was significantly increased when the podocytes were transfected with the KLF4 plasmid. As shown in Fig. 1B, C, F and G, KLF4 overexpression significantly decreased high glucose-induced podocyte apoptosis in line with the attenuation of cleaved caspase-3 expression. Moreover, KLF4 overexpression significantly reversed the disarrangement of F-actin, downregulated the expression of vimentin and α-SMA, and upregulated E-cadherin (Fig. 1D, F and G). Furthermore, KLF4 overexpression inhibited the decline in nephrin induced by DKD serum (Fig. 1E). These data demonstrate a crucial role for KLF4 in protecting against podocyte injury in a high glucose environment.

KLF4 overexpression protects against diabetic kidney damage in DKD mice. The western blotting results showed the level of KLF4 expression was increased in mouse renal tissues after lentiviral interference (Fig. 2A). The 24-h proteinuria, Scr and BUN were measured to analyze the effects on renal function. As shown in Fig. 2B, the transfer of the KLF4 plasmid resulted in an attenuation of proteinuria in DN mice 30 days after the injection. Scr and BUN were also decreased by the plasmid transfer of KLF4 compared with the vector-NC group (Scr in the vector-NC group, 0.78 0.02 μmol/l; Scr in the vector-KLF4 group, 0.70±0.02 μmol/l; P<0.05). PAS staining of the renal tissues showed that the glomeruli of DN mice had a greater diameter, mesangial matrix expansion and mesangial cell proliferation compared to that of the db/m mice. However, the aforementioned lesions of the glomeruli were attenuated following KLF4 plasmid injection compared to the vector-NC group (Fig. 2C).

Podocyte apoptosis and EMT biomarkers in the renal tissue were subsequently examined. The TUNEL staining results showed that the number of apoptotic cells was decreased in the vector-KLF4 group compared to the vector-NC group (Fig. 2E). The western blotting results showed that the KLF4 plasmid injection significantly reduced the expression of cleaved caspase-3 and α-SMA, and increased the expression of E-cadherin (Fig. 2D). Immunofluorescence double staining showed increased nephrin expression and attenuated vimentin expression in the vector-KLF4 group compared to the vector-NC group (Fig. 2F). These findings suggested that KLF4 has inhibitory effects on podocyte apoptosis and the progression of EMT in DN.

KLF4 overexpression upregulates podocyte autophagy to protect against diabetic kidney damage. To evaluate the role of autophagy in the protective effect of KLF4 against diabetic kidney damage, changes in autophagic markers were detected *in vivo* and *in vitro*. *In vitro*, the immunofluorescence results showed that treatment with DKD serum inhibited LC3 expression, but the LC3 fluorescence was substantially increased after the KLF4 plasmid transfer (Fig. 3A). In addition, the
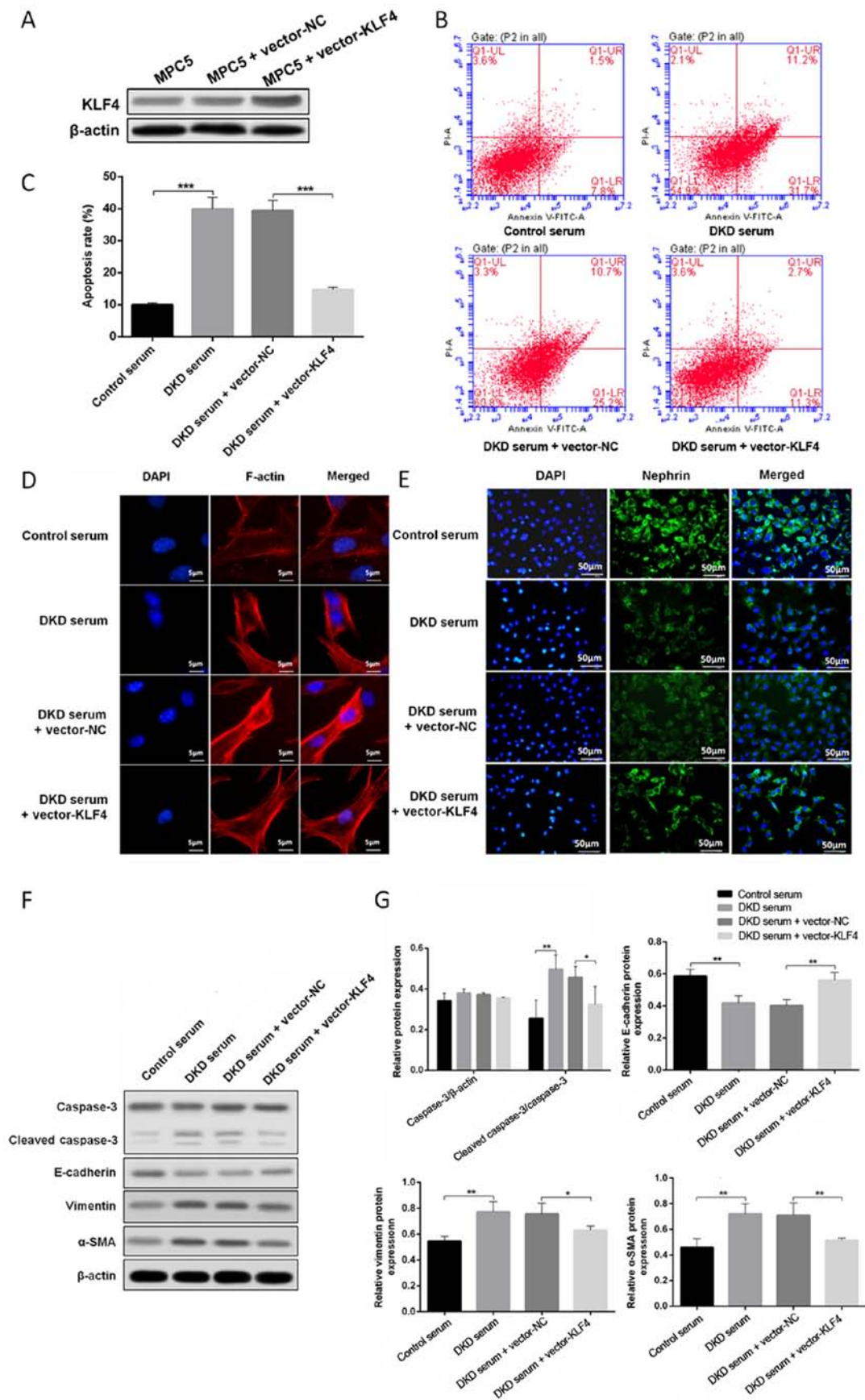
Figure 1. KLF4 overexpression protects against DKD mouse serum-induced podocyte injury. (A) Western blotting showing that transfection with the KLF4 plasmid increased KLF4 expression. (B) The representative images and (C) quantitative analysis of the apoptotic cells are presented for the individual groups. (D) Representative photomicrographs of F-actin immunofluorescence staining. Scale bars, 5 μm. (E) Representative photomicrographs of nephrin immunofluorescence staining. Scale bars, 50 μm. (F) Representative bands of caspase-3, cleaved-caspase-3, vimentin, α-SMA and E-cadherin protein expression in the individual groups. (G) Bar graphs showing the relative levels of protein expression. Data are presented as the mean ± SD (n=5). *P<0.05; **P<0.01; ***P<0.001. α-SMA, α-smooth muscle actin; KLF4, Krüppel-like factor 4; NC, negative control; PI, propidium iodide; DKD, diabetic kidney disease.
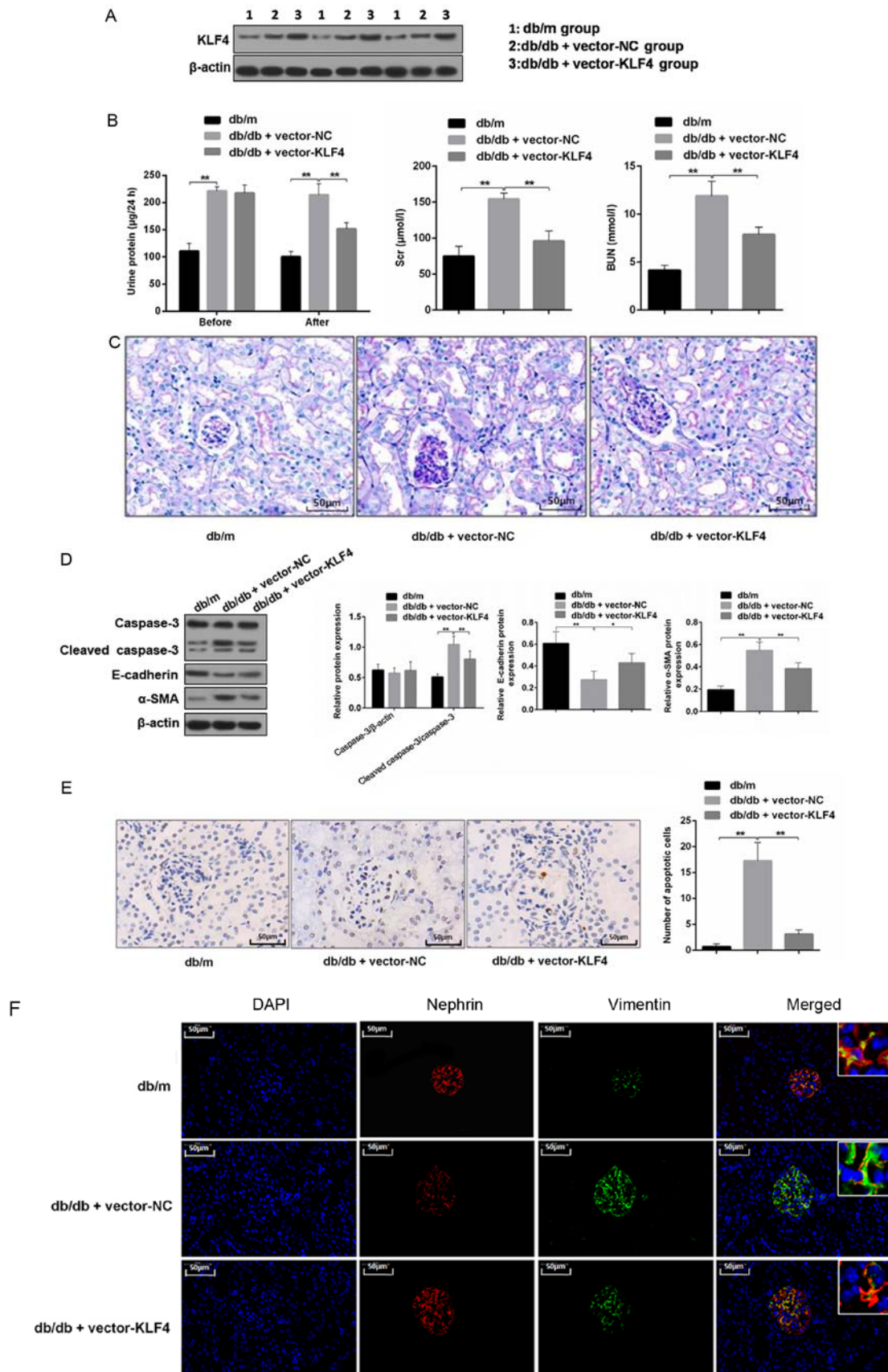
Figure 2. KLF4 overexpression protects against kidney damage in diabetic kidney disease model mice. (A) Representative bands of KLF4 in the individual groups. (B) Bar graphs showing the quantification of albuminuria, Scr and BUN in each group. (C) Representative photomicrographs of periodic acid-Schiff staining of the kidney tissues in each group. Scale bars, 50 μm. (D) Representative bands and quantitative evaluation of caspase-3, cleaved caspase-3, α-SMA and E-cadherin in the individual groups. (E) Representative photomicrographs and quantitative analysis of apoptotic cells via TUNEL staining of the kidney tissues in the individual groups. Scale bars, 50 μm. (F) Representative photomicrographs of immunofluorescence double staining of nephrin (red) and vimentin (green) in the individual groups. Scale bars, 50 μm. Data are presented as the mean ± SD (n=5). *P<0.05; **P<0.01. KLF4, Krüppel-like factor 4; BUN, blood urea nitrogen; Scr, serum creatinine; NC, negative control; α-SMA, α-smooth muscle actin.
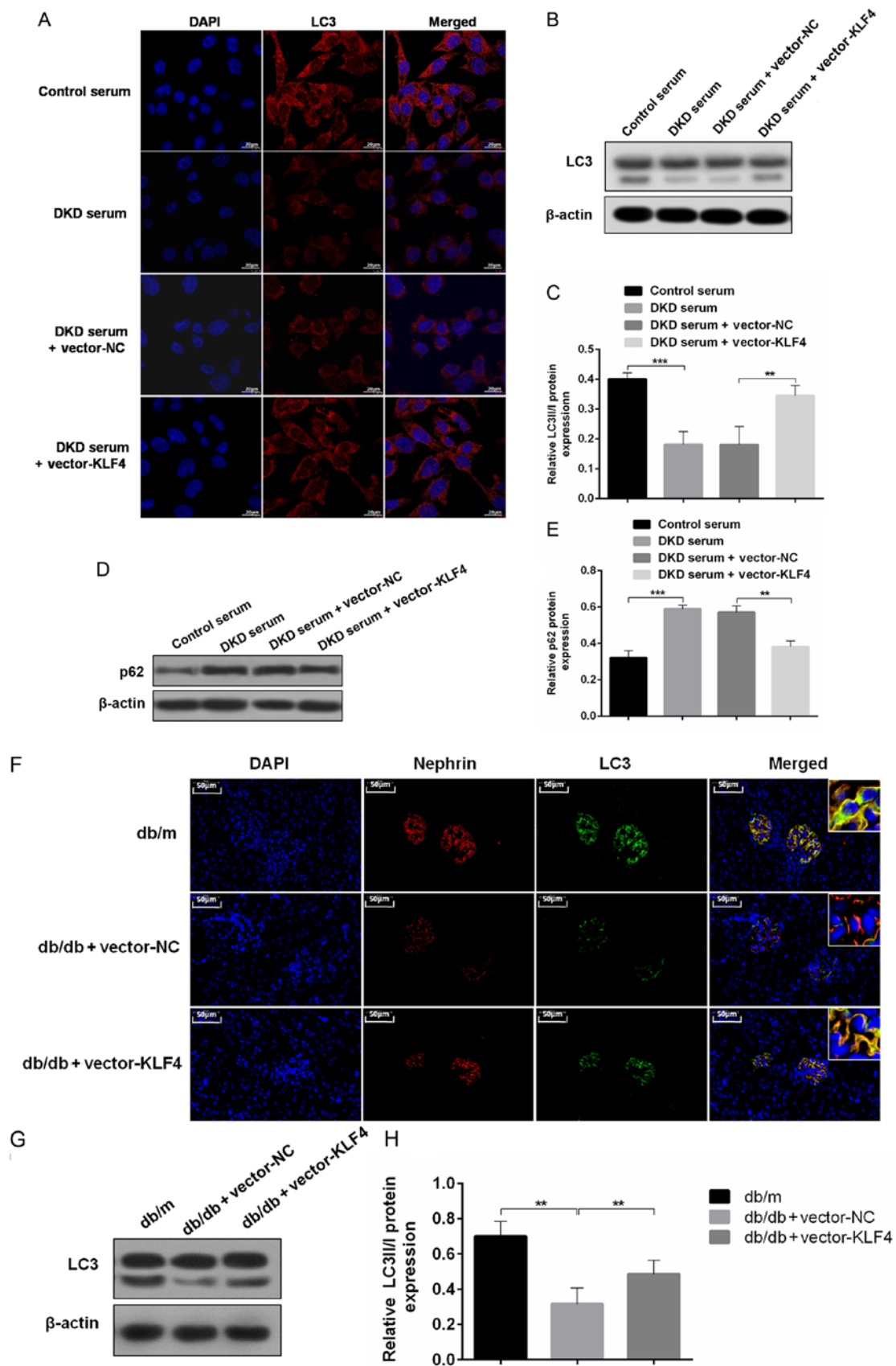
Figure 3. KLF4 overexpression upregulates podocyte autophagy both *in vivo* and *in vitro*. (A) Representative photomicrographs of *in vitro* LC3 immuno-fluorescence staining in the individual groups. Scale bars, 20 μm. (B) Representative bands of LC3 *in vitro* for each of the individual groups. (C) Bar graphs showing the relative quantification of LC3 *in vitro* for each of the individual groups. (D) Representative bands of p62 *in vitro* for each of the individual groups. (E) Bar graphs showing the relative quantification of p62 *in vitro* for each of the individual groups. (F) Representative photomicrographs of immunofluorescence double staining of nephrin (red) and LC3 (green) in the individual groups *in vivo*. Scale bars, 50 μm. (G) Representative bands of LC3 expression *in vivo* in each of the individual groups. (H) Bar graphs showing the relative quantification of LC3. Data are presented as the mean ± SD (n=5). **P<0.01; ***P<0.001. DKD, diabetic kidney disease; LC3, microtubule associated protein 1 light chain 3α; KLF4, Krüppel-like factor 4; NC, negative control.
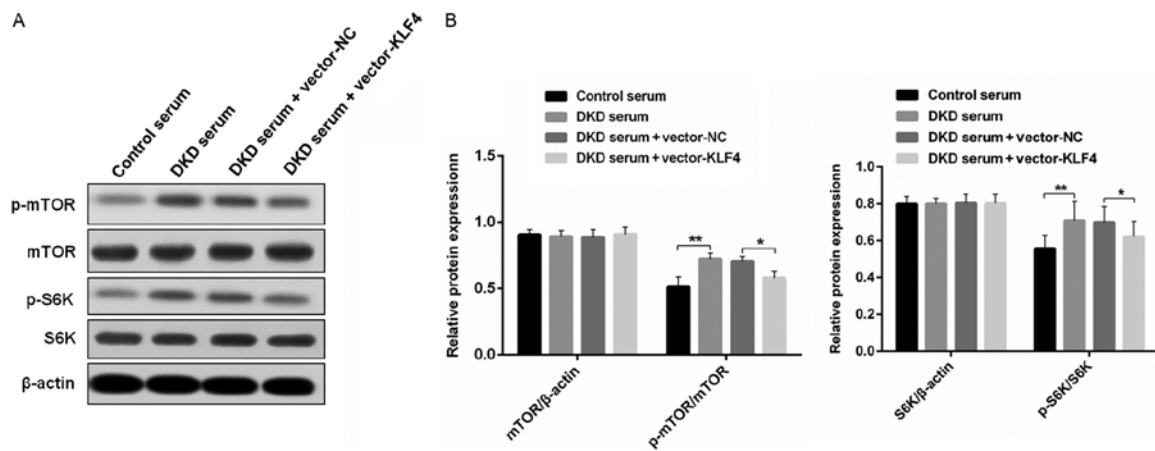
Figure 4. KLF4 overexpression inhibits the mTOR signaling pathway in podocytes treated with DKD mouse serum. (A) Representative bands of mTOR, S6K, p-mTOR and p-S6K expression in the individual groups. (B) Bar graphs showing the quantitative evaluation of the level of mTOR/β-actin, p-mTOR/mTOR, S6K/β-actin, and p-S6K/S6K in the individual groups. Data are presented as the mean ± SD (n=5). *P<0.05; **P<0.01. KLF4, Krüppel-like factor 4; p, phosphorylated; DKD, diabetic kidney disease; NC, negative control.

western blotting results demonstrated that KLF4 overexpression increased the LC3-II/LC3-I conversion and decreased p62 expression compared to the DKD serum group (Fig. 3B-E). Similar differences were observed in the *in vivo* studies. The LC3 fluorescence area was substantially increased following KLF4 plasmid injection in DKD mice, as shown by the immunofluorescence assay (Fig. 3F). Moreover, as shown in Fig. 3G and H, the LC3-II/LC3-I ratio was significantly increased in the vector-KLF4 group compared to the vector-NC group. Additionally, KLF4 overexpression increased the expression of nephrin compared to the vector-NC group (Fig. 3F). These data further demonstrated a crucial role for autophagy in modulating the protective effect of KLF4 against diabetic kidney damage.

KLF4 activates podocyte autophagy by negatively regulating the mTOR signaling pathway. To examine the mechanisms of KLF4-induced activation of podocyte autophagy, western blotting was performed to detect the level of relative protein expression in the mTOR signaling pathway *in vitro* (Fig. 4). It was found that there were similar levels of mTOR and S6K protein expression in each group; however, the overexpression of KLF4 resulted in a small but significant decrease in p-mTOR and p-S6K protein expression, which was increased in the DKD mouse serum group compared to the group treated with the control mouse serum.

Discussion

There is emerging evidence that KLFs play a vital role in the maintenance of normal renal function and are involved in key physiological processes in the kidneys (e.g., podocyte differentiation, tubulointerstitial inflammation and the progression of kidney fibrosis) (11,12). It was previously confirmed that KLF4 is primarily expressed in the podocytes of mice and humans, and its expression is decreased in both animal models and humans with a proteinuric status (8). In the present study, it was found that the overexpression of KLF4 significantly reduced the level of urinary albumin, Scr and BUN, whereas mesangial matrix expansion and mesangial cell proliferation were attenuated in DN mice. Furthermore, KLF4 overexpression

attenuated podocyte apoptosis and downregulated mesenchymal markers, accompanied by the upregulation of epithelial cell markers. Moreover, the present findings suggested that the overexpression of KLF4 may ameliorate DN by activating podocyte autophagy and inhibiting mTOR signaling.

Previous studies have shown that increased levels of urinary protein in DN are associated with podocyte injury, including podocyte apoptosis, detachment and EMT (13). In the present study, it was found that KLF4 overexpression significantly decreased the apoptosis rate of podocytes treated with DKD mouse serum and in DN mice, accompanied by a reduction in cleaved caspase-3, a crucial proteolytic cleavage enzyme in cellular apoptosis. These data suggested that KLF4 plays a protective role in podocytes. This role was confirmed by an increase in nephrin when KLF4 was upregulated in both the *in vivo* and *in vitro* experiments.

Podocyte EMT, which is characterized by the loss of epithelial cell markers (e.g., E-cadherin) and re-expression of mesenchymal markers (e.g., vimentin and α-SMA), is widely involved in the pathological process of DN (14). A previous study demonstrated that KLF4 overexpression attenuates lung fibrosis and EMT in transgenic mice (15). The present study found that KLF4 overexpression reversed the downregulation of E-cadherin, as well as the upregulation of both vimentin and α-SMA, in DN mouse podocytes. These results suggested that KLF4 is involved in the regulation of podocyte EMT in DN. This is in line with a recent study showing that matrix stiffness-regulated KLF5/KLF4 is related to the pathogenesis of renal fibrosis (16). However, the role of KLF4 in EMT remains controversial, especially in certain cancer studies (17,18). Thus, additional studies are required to clarify the precise relationship between KLF4 and EMT. In addition, renal histopathology demonstrated that mesangial matrix expansion and mesangial cell proliferation were alleviated in DN mice following the restoration of podocyte KLF4 expression in the present study. Previously, inflammation was found to play a central role in the progression of DN (19), and KLF4 has been reported to be a regulatory factor in lipopolysaccharide-induced inflammation and tissue damage, both *in vivo* and *in vitro* (20). Therefore, it was speculated that

the KLF4-mediated alleviation of the DN mouse pathological lesions may be associated with the regulation of inflammation, independent of suppressing podocyte apoptosis.

Autophagy is a major intracellular lysosomal degradation system and cellular process used to degrade and recycle proteins and other impaired cell organelles in lysosomes. Moreover, autophagy plays an important role in the maintenance of intracellular homeostasis. A study focusing on the potential effect of autophagy on kidney disease, including DN, was previously performed, indicating that the level of autophagy decreased in podocytes cultured in the serum of DN rats (21). In the past few years, numerous studies have suggested that the activation of autophagy in podocytes may be a potential therapy used to prevent the progression of DN (22,23). It has been shown that KLF4 regulates autophagy-associated gene expression by binding to the promoter regions of the sequestosome-1 gene encoding the p62 protein in multiple myeloma (24). The present study demonstrated that KLF4 overexpression increased the expression of the autophagy protein, LC3, and the LC3-II/LC3-I ratio, but decreased p62 expression in both DN mice and podocytes stimulated with high glucose serum, suggesting that the activation of autophagy may play an important role in ameliorating DKD associated with KLF4.

It has been well-established that the mTOR signaling pathway is involved in cellular growth, metabolism and the negative regulation of autophagy; however, the role of mTOR signaling in KLF4-mediated upregulation of autophagy in DN remains unknown. A previous study indicated that the transient silencing of KLF4 in mouse embryonic fibroblasts led to overactive mTOR activity, and autophagy activity was not restored when rapamycin reduced the level of mTOR (25). The present *in vitro* study demonstrated that the overexpression of KLF4 inhibited mTOR and S6K phosphorylation, an important downstream protein that leads to the activation of the mTORC1 pathway. The present findings suggested that KLF4 plays a negative regulatory role in podocyte mTOR signaling pathways.

In conclusion, the findings of the present study indicated that KLF4 plays a renoprotective role in diabetic renal injury, which is associated with the activation of podocyte autophagy. It was further demonstrated that KLF4 overexpression inhibited the mTOR/S6K signaling pathway. Therefore, the activation of podocyte autophagy and inactivation of mTOR/S6K signaling pathway via KLF4 may be an effective strategy for the treatment of DN.

Acknowledgements

Not applicable.

Availability of data and materials

The datasets analyzed during the current study are avaiable from the corresponding auhtor on reasonable request.

Authors' contributions

JJ and QH designed the study. YL proofread the article and participated in data analysis. HZ and JG performed the experiments. WZ performed the statistical analyses. JG wrote the manuscript. The final version of the manuscript was approved by all authors.

Ethics approval and consent to participate

This study was approved by the local ethics committee of Zhejiang Provincial People's Hospital. The study was performed in accordance with the UK Animals (Scientific Procedures) Act, 1986 and associated guidelines, and the EU Directive 2010/63/EU for animal experiments.

Patient consent for publication

Not applicable.

Competing interests

The authors declare that they have no competing interests.

References

1. Cunningham A, Benediktsson H, Muruve DA, Hildebrand AM and Ravani P: Trends in biopsy-based diagnosis of kidney disease: A population study. Can J Kidney Health Dis 5: 2054358118799690, 2018.
2. Huang YM, Xu D, Long J, Shi Y, Zhang L, Wang H, Levin A and Zhao MH: The spectrum of chronic kidney disease in China: A national study based on hospitalized patients from 2010 to 2015. Nephrology (Carlton) 24: 725-736, 2019.
3. Pontrelli P, Oranger A, Barozzino M, Divella C, Conserva F, Fiore MG, Rossi R, Papale M, Castellano G, Simone S, *et al*: Deregulation of autophagy under hyperglycemic conditions is dependent on increased lysine 63 ubiquitination: A candidate mechanism in the progression of diabetic nephropathy. J Mol Med (Berl) 96: 645-659, 2018.
4. Dai H, Liu Q and Liu B: Research progress on mechanism of podocyte depletion in diabetic nephropathy. J Diabetes Res 2017: 2615286, 2017.
5. Yamaguchi Y, Iwano M, Suzuki D, Nakatani K, Kimura K, Harada K, Kubo A, Akai Y, Toyoda M, Kanauchi M, *et al*: Epithelial-mesenchymal transition as a potential explanation for podocyte depletion in diabetic nephropathy. Am J Kidney Dis 54: 653-664, 2009.
6. Ghaleb AM and Yang VW: Krüppel-like factor 4 (KLF4): What we currently know. Gene 611: 27-37, 2017.
7. Yoshida T, Yamashita M, Iwai M and Hayashi M: Endothelial krüppel-like factor 4 mediates the protective effect of statins against ischemic AKI. J Am Soc Nephrol 27: 1379-1388, 2016.
8. Hayashi K, Sasamura H, Nakamura M, Azegami T, Oguchi H, Sakamaki Y and Itoh H: KLF4-dependent epigenetic remodeling modulates podocyte phenotypes and attenuates proteinuria. J Clin Invest 124: 2523-2537, 2014.
9. Gong J, Jin J, Zhao L, Li Y, Li Y and He Q: Tripterygium glycoside protects against puromycin amino nucleoside-induced podocyte injury by upregulating autophagy. Int J Mol Med 42: 115-122, 2018.
10. Tesch GH and Lim AK: Recent insights into diabetic renal injury from the db/db mouse model of type 2 diabetic nephropathy. Am J Physiol Renal Physiol 300: F301-F3010, 2011.

11. Mallipattu SK, Guo Y, Revelo MP, Roa-Peña L, Miller T, Ling J, Shankland SJ, Bialkowska AB, Ly V, Estrada C, *et al*: Krüppel-Like factor 15 mediates glucocorticoid-induced restoration of podocyte differentiation markers. J Am Soc Nephrol 28: 166-184, 2017.
12. Mallipattu SK, Estrada CC and He JC: The critical role of Krüppel-like factors in kidney disease. Am J Physiol Renal Physiol 312: F259-F265, 2017.
13. Vogelmann SU, Nelson WJ, Myers BD and Lemley KV: Urinary excretion of viable podocytes in health and renal disease. Am J Physiol Renal Physiol 285: F40-F48, 2003.
14. Loeffler I and Wolf G: Epithelial-to-mesenchymal transition in diabetic nephropathy: Fact or fiction. Cells 4: 631-652, 2015.
15. Lin L, Han Q, Xiong Y, Li T, Liu Z, Xu H, Wu Y, Wang N and Liu X: Krüpple-like-factor 4 attenuates lung fibrosis via inhibiting epithelial-mesenchymal transition. Sci Rep 7: 15847, 2017.
16. Chen WC, Lin HH and Tang MJ: Matrix-stiffness-regulated inverse expression of Krüppel-like factor 5 and Krüppel-like factor 4 in the pathogenesis of renal fibrosis. Am J Pathol 185: 2468-2481, 2015.
17. Pinho AV, Rooman I and Real FX: p53-dependent regulation of growth, epithelial-mesenchymal transition and stemness in normal pancreatic epithelial cells. Cell Cycle 10: 1312-1321, 2011.
18. Dong P, Kaneuchi M, Watari H, Hamada J, Sudo S, Ju J and Sakuragi N: MicroRNA-194 inhibits epithelial to mesenchymal transition of endometrial cancer cells by targeting oncogene BMI-1. Mol Cancer 10: 99, 2011.
19. Wada J and Makino H: Inflammation and the pathogenesis of diabetic nephropathy. Clin Sci (Lond) 124: 139-152, 2013.
20. Li Z, Jia Y, Han S, Wang X, Han F, Zhang J, Zhang W, Guan H and Hu D: Klf4 alleviates lipopolysaccharide-induced inflammation by inducing expression of MCP-1 induced protein 1 to deubiquitinate TRAF6. Cell Physiol Biochem 47: 2278-2290, 2018.
21. Jin J, Wu D, Zhao L Zou W, Shen W, Tu Q and He Q: Effect of autophagy and stromal interaction molecule 1 on podocyte epithelial-mesenchymal transition in diabetic nephropathy. Int J Clin Exp Pathol 5: 2450-2459, 2018.
22. Lenoir O, Jasiek M, Hénique C, Guyonnet L, Hartleben B, Bork T, Chipont A, Flosseau K, Bensaada I, Schmitt A, *et al*: Endothelial cell and podocyte autophagy synergistically protect from diabetes-induced glomerulosclerosis. Autophagy 11: 1130-1145, 2015.
23. Tagawa A, Yasuda M, Kume S, Yamahara K, Nakazawa J, Chin-Kanasaki M, Araki H, Araki S, Koya D, Asanuma K, *et al*: Impaired podocyte autophagy exacerbates proteinuria in diabetic nephropathy. Diabetes 65: 755-767, 2016.
24. Riz I, Hawley TS and Hawley RG: KLF4-SQSTM1/p62-associated prosurvival autophagy contributes to carfilzomib resistance in multiple myeloma models. Oncotarget 6: 14814-14831, 2015.
25. Liu C, DeRoo EP, Stecyk C, Wolsey M, Szuchnicki M and Hagos EG: Impaired autophagy in mouse embryonic fibroblasts null for Krüppel-like Factor 4 promotes DNA damage and increases apoptosis upon serum starvation. Mol Cancer 14: 101, 2015.